18TH WORLD CONFERENCE ON EARTHQUAKE ENGINEERING
WCEE2024
MILAN

MILAN, ITALY
30TH JUNE - 5TH JULY 2024

www.wcee2024.it

SEISMIC PERFORMANCE OF EXPOSED COLUMN-BASE PLATE CONNECTIONS IN EXISTING STEEL FRAMES

L. Di Sarno[1], J.-R. Wu[2], N. Stathas[3], F. Freddi[2], M. D'Aniello[4], S. Bousias[3], R. Landolfo[4] & E. M. Güneyisi[5]

[1] University of Liverpool, Liverpool, United Kingdom, luigi.di-sarno@liverpool.ac.uk

[2] University College London, London, United Kingdom

[3] University of Patras, Patras, Greece

[4] University of Naples Federico II, Naples, Italy

[5] Gaziantep University, Gaziantep, Turkey

Abstract: *Existing steel frames not conforming to modern seismic design codes are typically vulnerable to earthquakes due to inadequate seismic detailing. This type of structure is commonly equipped with exposed column-base connections that are usually semi-rigid and/or partial strength. Therefore, their behaviour may significantly affect the seismic performance of the structure. However, current code provisions provide limited recommendations for the seismic performance assessment and retrofit of exposed column-base connections in existing frames. The ERIES HIT-BASE (Earthquake Assessment of Base-Column Connections in Existing Steel Frames) project aims to experimentally investigate the performance of existing steel frames with exposed column-base plate connections subjected to earthquake sequences. A non-seismically designed steel frame is used as case study building to conduct bi-directional pseudo-dynamic tests at the STRULAB-RW at the University of Patras, Greece. The performance of two types of column-base plate connections, i.e., stiffened and unstiffened, respectively representing the base connections of an external moment-resisting frame and an internal gravity frame, are investigated. Preliminary numerical simulations on a simplified model developed in OpenSees were carried out to support the design of the specimen, the loading protocol and seismic intensities to be used during the test. This paper introduces the motivations and objectives of the project, the preparatory work done to design the experimental work, the dynamic identification and the preliminary results of pseudo-dynamic tests of the experimental mockup.*

1 Introduction

The poor performance of column-base connections in existing steel frames experienced after severe seismic events has highlighted the need for an improved understanding of their response (*e.g.,* Mahin, 1998; Clifton *et al.,* 2011; Okazaki *et al.,* 2013; Di Sarno *et al.,* 2018, Gutiérrez-Urzúa *et al.,* 2021). Column-base connections are usually required to sustain simultaneously axial forces, shear forces and bending moments and transfer the loads from the superstructure to the foundation. Previous research has investigated the behaviour of various types of column-base connections, including exposed base plate connections (*e.g.,* Latour *et al.,* 2014; Fasaee *et al.,* 2018; You and Lee, 2020) and embedded connections (*e.g.,* Di Sarno *et al.,* 2007; Grilli *et al.,* 2017; Inamasu *et al.,* 2021). The former have conventionally been used in many European countries for low-

to-medium rise steel frames, which consist of tapered steel plates welded onto the column-base plates and anchored to the foundation block through steel bolted bars. Triangular stiffeners are also frequently used to enhance the rigidity of connections. Figure 1 schematically shows the layout of typical exposed column-base plate connections and their possible failure mechanisms.

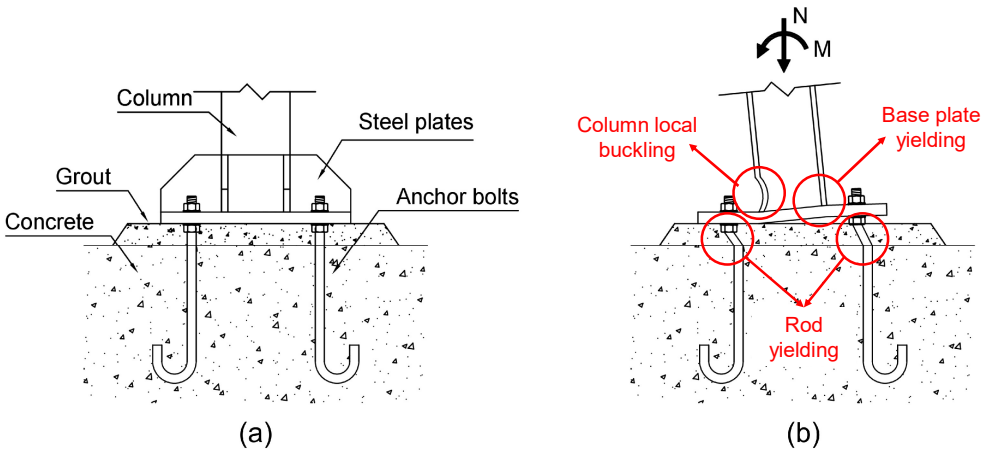

Figure 1. Conventional exposed column-base plate connection in steel frames: (a) typical layout; (b) possible failure mechanisms.

The current European codes provide limited guidance on the assessment and retrofitting of exposed base plate connections. For example, the assessment framework for existing structures, *i.e.,* the Eurocode 8-Part 3 (EC8-3) (CEN, 2005c), primarily accounts for steel beam-to-column connections and does not contain explicit guidance for column-base connections. On the other hand, the component approach adopted in the Eurocode 3-Part 1.8 (EC3-1.8) (CEN, 2005b) mainly deals with the prediction of the rotational stiffness and moment capacity of exposed base plate connections. Nonetheless, it does not cover the whole moment-rotation relationship, which requires a proper definition of the ultimate deformation capacity of the connections (Latour *et al.,* 2014).

Despite the great effort that has been put into the research of column-base connections, the number of existing experimental tests is still limited, the majority of which have focused on testing exposed column-base connections subjected to uniaxial bending (*e.g.,* Zhou *et al.,* 2004; Lee *et al.,* 2008a; 2008b; Kanvinde *et al.,* 2012; Borzouie *et al.,* 2015; 2016), with a few recent experimental studies focusing on exposed base plate connections under biaxial bending (*e.g.,* Cloete and Roth, 2021; Seco *et al.,* 2021). Nevertheless, the performance of column-base plate connections has rarely been investigated through testing full-scale steel frames under bi-directional loading. Moreover, the influence of the cumulative damage in such column bases due to repeated earthquakes has received limited attention.

To address the aforementioned issues, the ERIES HIT-BASE (Earthquake Assessment of Base-Column Connections in Existing Steel Frames) project aims to experimentally investigate the performance of existing steel frames subjected to earthquake sequences, paying particular attention to the behaviour of conventional exposed column-base plate connections. The tests focus on a large-scale specimen and account for the bi-directional loading inducing axial forces, bi-directional shear forces, bending moments, and torsion to the column base connections. A non-seismically designed steel frame is employed as the case study building for the bi-directional pseudo-dynamic (PsD) tests at the STRULAB-RW at the University of Patras, Greece. The performance of two types of column-base plate connections is investigated, *i.e.,* stiffened and unstiffened, respectively representing the base connections of an external moment-resisting frame and an internal gravity frame. Preliminary numerical simulations were carried out to support the design of the specimen and the testing programme using a simplified model developed in OpenSees. This paper introduces the motivations and objectives of the project, the preparatory work done to design the experimental work, the dynamic identification and the preliminary results of PsD tests of the specimen.

2 Case study structure

2.1 Description of the case study structure

The case study building is a two-storey, three-bay by three-bay steel frame, whose layout and section views are presented in Figure 2. Each storey of the steel frame is 2.75 m in height, and the bay spans 5.5 and 3.5 m in the longitudinal and transverse directions, respectively. The building was primarily designed for gravity loads following the European design code Eurocode 3 (EC3) (CEN, 2005a) and without sufficient seismic detailing. The gravity design was carried out considering the self-weight of partitions, equal to 0.5 kN/m^2, and an imposed load of 3 kN/m^2. This led to the steel profiles HE140 and HE160 for perimeter and internal columns, respectively, using S355 steel, which has a characteristic yield stress of 355 MPa. Moreover, the composite slab has a depth of 250 mm and is made of C20/25 concrete and grade B450C reinforcement. It is worth noting that the bases of all perimeter columns were designed to be fixed connections to simulate the external moment-resisting frames, as shown by the section views in Figure 2. In contrast, those of internal columns were pinned connections, representing internal gravity frames.

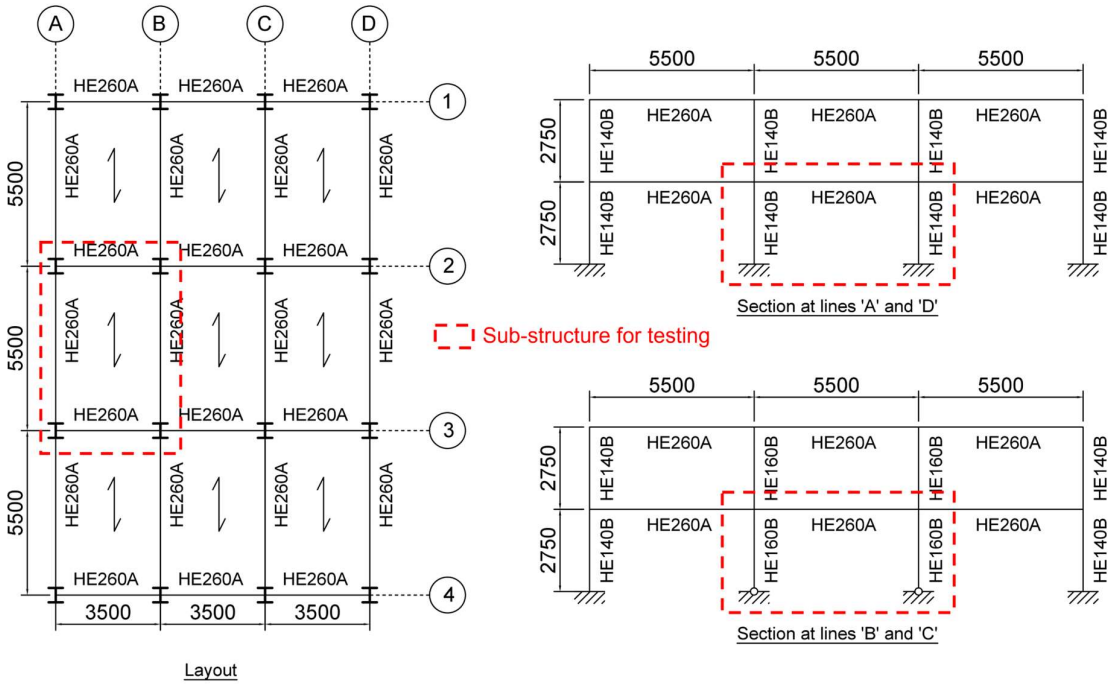

Figure 2. Layout and section views of the case study steel frame (unit: mm).

2.2 Description of the mockup

The test mockup is a sub-structure of the case study building, as depicted in Figure 3, which is a single-storey, single-bay steel frame spanning 5.5 and 3.5 m in the longitudinal and transverse directions, respectively, and storey heights of 2.75 m. S355 steel grade was used for structural steel components, B450C reinforcing steel bars and C20/25 concrete for the composite slab. Figure 4 shows the specimen at the STRULAB-RW at the University of Patras and some details of the connections. The pictures represent the frame under construction before grouting underneath steel base plates. As this project aims to investigate the behaviour of column-base plate connections, concrete footings supporting each column-base connection were also constructed in the lab. For consistency, the footings are also made of C20/25 concrete reinforced by B450C steel bars. Two types of column-base plate connections were employed, *i.e.,* stiffened and unstiffened, corresponding to the fixed and pinned connections in Figure 3, respectively. Lastly, additional concrete blocks (see Figure 4) are placed on the composite slab to account for the mass of non-structural components, *i.e.,* the partition walls and the imposed load considered in the gravity design of the case study building in the previous section, as well as the equivalent masses from the second storey.

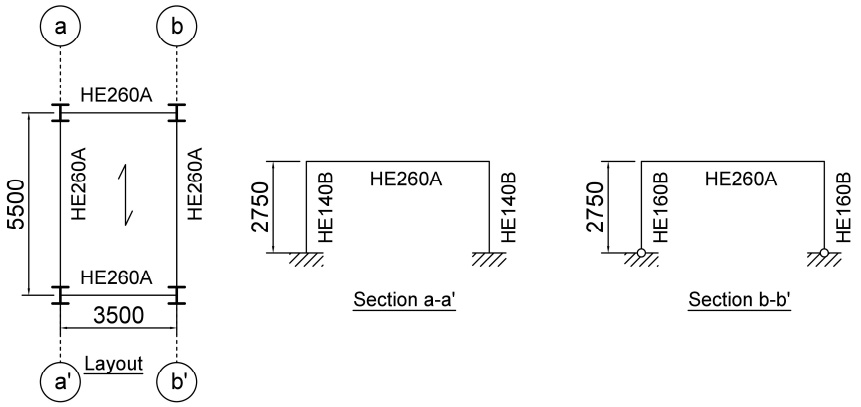

Figure 3. Dimensions of the test specimen (unit: mm).

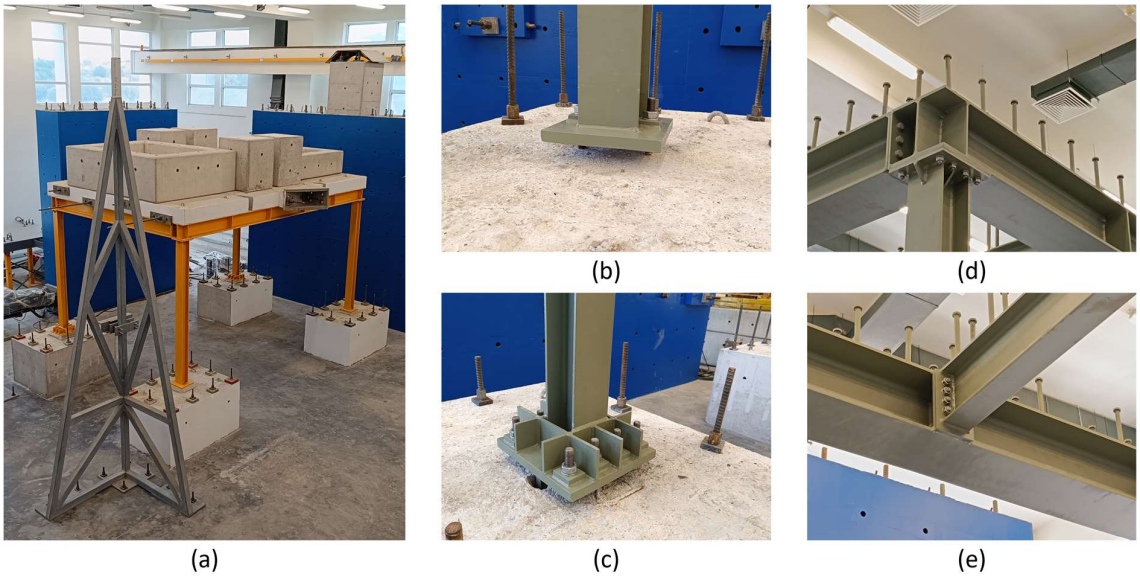

Figure 4. Construction details of the specimen: (a) overview of the mock-up; (b) unstiffened base connection; (c) stiffened base connection; (d) beam-to-column connection; (e) beam-to-beam connection.

3 Numerical simulations and test design

3.1 Finite Element (FE) modelling of the mockup

A preliminary Finite Element (FE) model of the mockup was developed in OpenSees (McKenna *et al.,* 2010) to predict the response of the structure and to enable the design of experimental tests. Figure 5 shows a schematic view of the model. The columns were modelled using force-based elements along with the 'Steel02' uniaxial material model with Young's modulus of 210 GPa and yield stress of 406 MPa, which were calibrated based on previous coupon tests (Di Sarno *et al.,* 2021). Conversely, beams were assumed to remain elastic during the analysis and hence modelled using elastic beam elements. Beam-to-column connections were considered fully rigid due to the welded connection type and the stiffeners placed at the joints (see Figure 4d). The perimeter columns (HE140) were fixed at the base to simulate the stiffened base connections, while the internal columns (HE160) were pinned to simulate the unstiffened base connections. Additionally, a rigid diaphragm multi-point constraint was also implemented at the floor level to account for the effects of the composite slab. It is worth mentioning that the modelling strategies for the column-base connections are very simplified in the current model. However, they have been considered suitable to support the decisions required for the design of the tests and will be updated successively by comprehensive model validation against the test results.

To facilitate the subsequent modal, pushover and dynamic analyses, an equivalent mass of 29.59 tons was equally distributed and lumped at the four slab nodes, accounting for the mock-up's self-weight, the weight of non-structural components, the imposed load, and all the relevant gravity loads from the second floor. In addition, the gravity loads were applied at those slab nodes as concentrated loads, as illustrated in Figure 5. It is also worth noting that a damping ratio of 3% was assumed to facilitate the dynamic analysis.

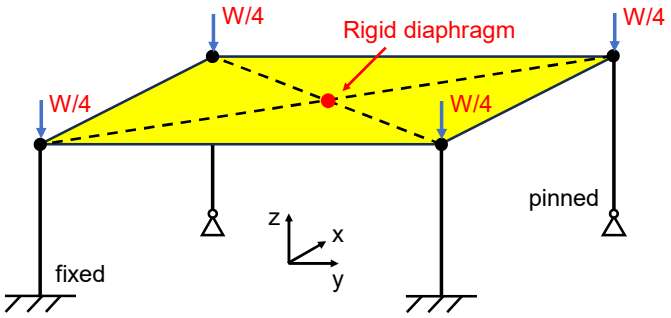

Figure 5. Schematic view of the FE model of the steel frame specimen in OpenSees.

3.2 Modal characterisation and free vibration tests

Modal analysis was performed to estimate the specimen's modal properties. The natural periods and mode shapes corresponding to the first three vibration modes obtained from the FE model are presented in Table 1. It can be observed that the first mode is purely translational along the *x*-direction (see Figure 5), while the following two are torsional modes due to the structural asymmetry caused by the pinned and fixed ends at column bases.

Table 1. Modal properties of the steel frame specimen estimated by the Finite Element (FE) model.

	1st mode	2nd mode	3rd mode
Period (sec)	0.82	0.76	0.49
Mode shape	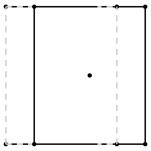	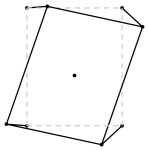	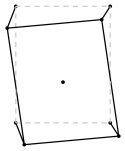

The modal properties of the specimen were also determined experimentally through free vibration tests, which were carried out by applying initial displacement at the slab level independently in the *x*- and *y*-directions and then releasing the force to allow free vibration of the structure. Accelerations of the slab along *x*- and *y*-directions were monitored during the free vibration, and the corresponding Fast Fourier Transform (FFT) spectra are presented in Figure 6. A total of three modes can be identified from the FFT spectra, as indicated by the three peaks in the spectra. The single peak shown in Figure 6a represents a translational mode in the *x*-direction, which has a period of 0.69 sec. In the meantime, the two peaks shown in Figure 6b represent a rotational mode of the specimen, as the spectra exhibit peaks in both the *x*- and *y*-directions. The periods associated with the two rotational modes are 0.62 and 0.38 sec, respectively. Although the FE model overestimated the natural periods of the specimen, which could be a limitation of the simplified modelling of the column-base connections, the predicted mode shapes agreed with the outcomes of the free vibration tests.

3.3 Pushover analysis and cyclic tests

Pushover analyses were performed on the FE model to predict the base shear capacity of the specimen along the *x*- and *y*-directions (see Figure 5), respectively. The capacity curves are presented in Figure 7, along with the measured response of the specimen under cyclic loading before yielding. It can be seen that the FE model had a base shear capacity of 106 and 233 kN in the *x*- and *y*-directions, respectively. Also, the FE model exhibited a lateral stiffness of around 1.62 kN/mm in the x-direction, which was over 30% less than the measured value (Figure 7a). A possible reason for this is that the unstiffened base connections possessed some flexural stiffness in this direction. In the *y*-direction, the FE model exhibited approximately the same

lateral stiffness as the specimen (Figure 7b), which was around 3.74 kN/mm. This is in general consistent with the findings from the comparisons between the results of modal analysis and free vibration tests, where the underestimated lateral stiffness in the *x*-direction led to overestimation of the natural periods for all the three vibration modes identified.

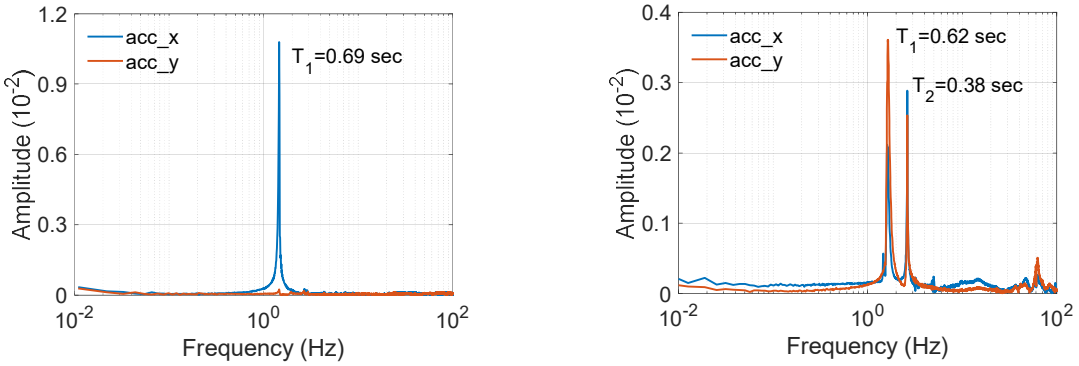

Figure 6. Natural periods determined from the free vibration tests in (a) x- and (b) y-direction (see Figure 5).

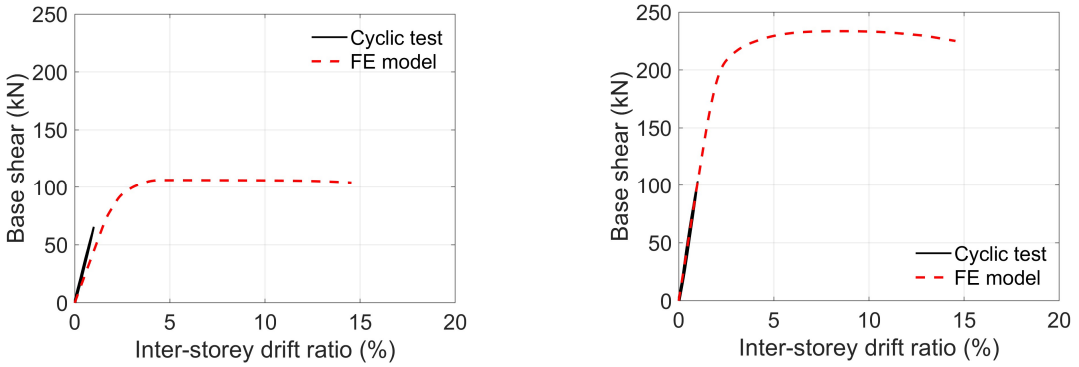

Figure 7. Capacity curves and measured response of the steel frame specimen during cyclic loading in (a) x- and (b) y-direction (see Figure 5).

3.4 Record selection for pseudo-dynamic (PsD) tests

The records of two ground motions referring to the 2016 Central Italy earthquakes were selected for performing PsD tests. Records of both horizontal components of the selected ground motions were extracted from the Engineering Strong-Motion Database (ESM) (Luzi *et al.,* 2016) to enable the bi-direction PsD tests. Some basic information about the selected ground motion records, including date, moment magnitude (M_w) and epicentral distance (R_{epi}) of the seismic event, are summarised in Table 2, while the accelerograms and corresponding response spectra for 3% damping are presented in Figure 8. The selected ground motions are characterised by PGA of 0.37g and 0.37g in the North-South (N-S) direction, while by PGA of 0.35g and 0.48g in the East-West (E-W) direction. It can also be seen from the acceleration spectra that the selected ground motions exhibit relatively large spectral acceleration at the natural periods of the specimen identified through the free vibration tests, *i.e.,* 0.69, 0.62 and 0.38 sec.

Table 2. Basic information of the selected ground motions for PsD tests.

	Event ID	Date & Hour	M_W (-)	R_{epi} (km)
GM1	EMSC-20160824_0000006	24/08/2016 at 1.36	6.0	15.3
GM2	EMSC-20161030_0000029	30/10/2016 at 6.40	6.5	4.6

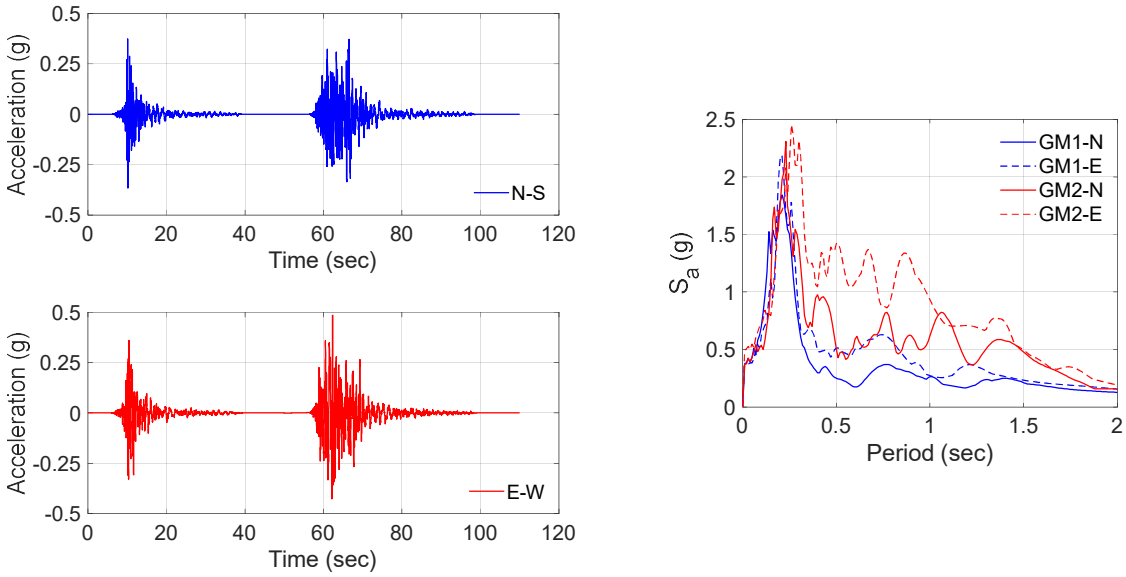

Figure 8. Selection of ground motion records: (a) the accelerograms in both the N-S and E-W direction; (b) acceleration spectra for 5% damping.

3.5 Prediction of the seismic response

The response of the specimen subjected to the selected ground motion records was predicted by performing non-linear time-history analyses on the FE model. Two load cases (LC) were considered for the application of the horizontal components of selected ground motions. LC1 corresponds to the FE model with *x*-axis in the E-W direction and *y*-axis in the N-S direction, while LC2 corresponds to the FE model with *x*-axis in the N-S direction and *y*-axis in the E-W direction. Moreover, two scaling factors (SF), equal to 1.0 and 1.5, were considered for the dynamic analysis, aiming to cause inelastic deformation of the specimen.

The results of the non-linear dynamic analysis are presented in Figure 9 and Figure 10. It can be seen in Figure 9 that for SF=1.0, the model only exhibited slight inelastic deformation in the *x*-direction in the case of LC1, while it remained elastic in both *x*- and *y*-directions in the case of LC2. The peak inter-storey drift ratios (IDRs) achieved for LC1 were 4.53% and 0.99% in the *x*- and *y*-direction, respectively. For LC2, the peak IDRs were 3.15% and 2.77% in the *x*- and *y*-direction. On the other hand, as shown in Figure 10, for the case of SF=1.5, the model exhibited more significant inelastic deformation in the *x*-direction, regardless of the load cases. The peak IDRs achieved for LC1 were 6.34% and 1.93% in the *x*- and *y*-direction, respectively. For LC2, the peak IDRs were 6.91% and 4.28% in the *x*- and *y*-direction. These preliminary results also led to the conclusion that LC2 was more detrimental than LC1, hence the former was adopted for the PsD tests.

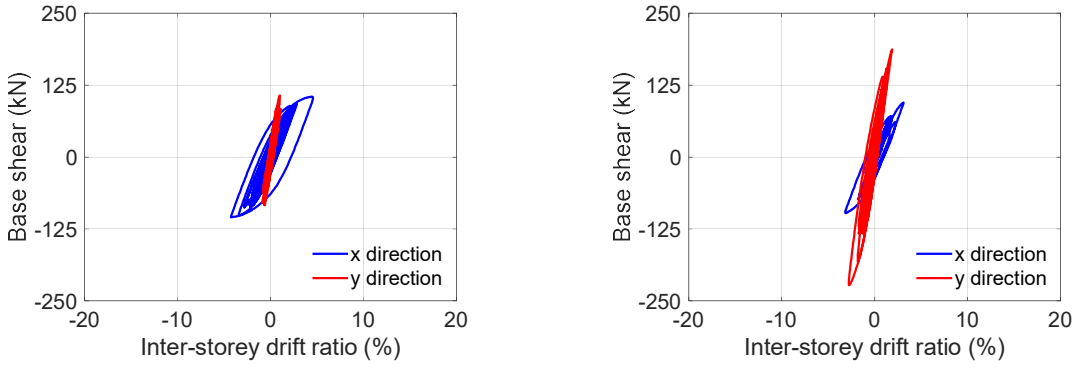

Figure 9. Estimated response of the specimen with SF=1.0: (a) LC1; (b) LC2.

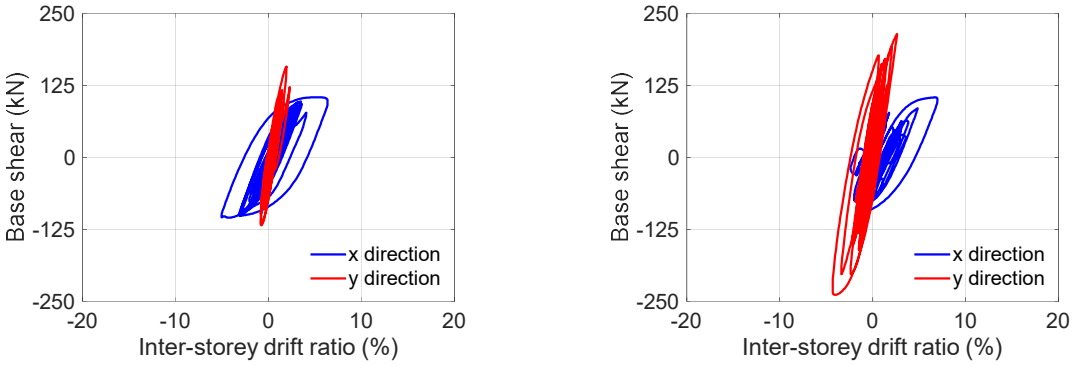

Figure 10. Estimated response of the specimen with SF=1.5: (a) LC1; (b) LC2.

3.6 Preliminary outcomes of the PsD tests

The results of the PsD tests for SF=1.0, including the hysteretic response of the test specimen and the rotation of slab, are presented Figure 11 in comparison with the predictions from the FE model. It can be seen that the specimen did not exhibit significant inelastic behaviour during the test and showed a greater stiffness in the *x*-direction than the FE model. The peak IDR recorded in this direction was approximately 2.69% and 3.15% in the positive and negative direction, respectively. Correspondingly, the FE model provided an estimate of the peak IDR equal to 2.97% and 3.33%, respectively, in the positive and negative *x*-direction, resulting in around 5-10% overestimation of the peak IDR.

On the other hand, as shown in Figure 11b, the specimen exhibited some pinching effects in the *y*-direction, due to the damage in column base connections (*e.g.,* cracking of the concrete base). The peak IDR recorded in this direction was approximately 2.24% and 3.11% in the positive and negative direction, respectively. The corresponding predictions from the FE model were 1.85% and 2.81%. It is also evident that the FE model, although having similar stiffness in the *y*-direction to the specimen (see Figure 7), underestimated the peak IDR by as much as 20%, due to the simplification of the base connections in the FE model, which failed to account for the pinching effects.

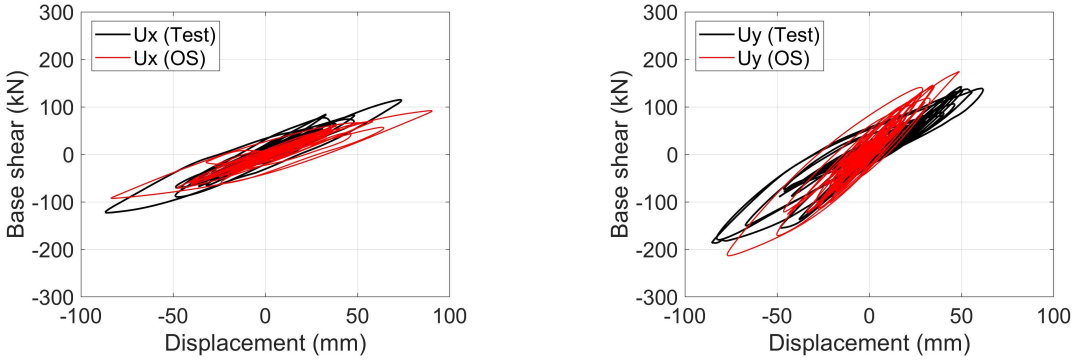

Figure 11. Hysteretic response of the specimen obtained from tests with SF=1.0 measured at the centroid of the slab: (a) in x-direction; (b) in y-direction.

4 Conclusions

This paper presents the preparatory work carried out for the experimental campaign of the ERIES HIT-BASE project and some preliminary results. The project aims to perform large-scale bi-directional PsD tests on a steel frame to investigate the seismic response of conventional exposed column-base plate connections. A preliminary and simplified FE model of the specimen was developed in OpenSees to support the test design. The preliminary FE results, including modal properties and capacity curves, were predicted and compared with

the outcomes of the characterisation tests of the specimen, *i.e.,* free vibration and elastic cyclic tests. The numerical predictions satisfacoty match the experimental results. However, the rigidity of the numerical model in *x*-direction is slightly smaller than the experimental one because of the simplified assumptions of the unstiffened base-connection (*i.e.,* pinned in the model). Nevertheless, the FE model was considered adequate to support the design of the tests. After validation, such FE model has been used to evaluate the response of the specimen under the selected ground motion records for the PsD tests. Two scaling factors (*i.e.,* 1.0 and 1.5) were eventually decided based on the results of dynamic analysis to induce the inelastic deformation of interest during the PsD tests.

5 Acknowledgements

This work is supported by the Engineering Research Infrastructures for European Synergies (ERIES) project (www.eries.eu), which has received funding from the European Union's Horizon Europe Framework Programme under Grant Agreement No. 101058684. This is ERIES publication number C13.

6 References

Borzouie J., MacRae G.A., Chase J.G., Rodgers G.W., Clifton G.C. (2015). Experimental studies on cyclic performance of column base weak axis aligned asymmetric friction connection, *Journal of Constructional Steel Research*, 112: 252-262.

Borzouie J., MacRae G.A., Chase J.G., Rodgers G.W., Clifton G.C. (2016). Experimental studies on cyclic performance of column base strong axis–aligned asymmetric friction connections, *Journal of Structural Engineering*, 142(1): 04015078.

CEN (2005a). *EN 1993-1-1:2005. Eurocode 3: Design of steel structures. Part 1-1: General rules and rules for buildings*, Comité Européen de Normalisation, Brussels.

CEN (2005b). *EN 1993-1-8:2005. Eurocode 3: Design of steel structures. Part 1-8: Design of joints*, Comité Européen de Normalisation, Brussels.

CEN (2005c). *EN 1998-1:2005. Eurocode 8: Design of structures for earthquake resistance - Part 1: General rules, seismic actions and rules for buildings*, Comité Européen de Normalisation, Brussels.

Clifton C., Bruneau M., MacRae G., Leon R., Fussell A. (2011). Steel structures damage from the Christchurch earthquake series of 2010 and 2011, *Bulletin of the New Zealand Society for Earthquake Engineering*, 44(4): 297-318.

Cloete R., Roth C.P. (2021). Column base connections under compression and biaxial moments: Experimental and numerical investigations, *Journal of Constructional Steel Research*, 184: 106834.

Di Sarno L., Freddi F., D'Aniello M., Kwon O.-S., Wu J.-R., Gutiérrez-Urzúa F., Landolfo R., Park J., Palios X., Strepelias E. (2021). Assessment of existing steel frames: Numerical study, pseudo-dynamic testing and influence of masonry infills. *Journal of Constructional Steel Research*, 185: 106873.

Di Sarno L., Paolacci F., Sextos A.G. (2018). Seismic performance assessment of existing steel buildings: a case study, *Key Engineering Materials*, 763: 1067-1076.

Di Sarno L., Pecce M.R., Fabbrocino G. (2007). Inelastic response of composite steel and concrete base column connections, *Journal of Constructional Steel Research*, 63(6): 819-832.

Fasaee M.A., Banan M.R., Ghazizadeh S. (2018). Capacity of exposed column base connections subjected to uniaxial and biaxial bending moments, *Journal of Constructional Steel Research*, 148: 361-370.

Grilli D., Jones R., Kanvinde A. (2017). Seismic performance of embedded column base connections subjected to axial and lateral loads, *Journal of Structural Engineering*, 143(5): 04017010.

Gutiérrez-Urzúa, L.F., Freddi, F., Di Sarno, L. (2021). Comparative analysis of code based approaches for the seismic assessment of existing steel moment resisting frames, *Journal of Constructional Steel Research*, 181: 106589.

Kanvinde A.M., Grilli D.A., Zareian F. (2012). Rotational stiffness of exposed column base connections: Experiments and analytical models, *Journal of Structural Engineering*, 138(5): 549-560.

Inamasu H., Kanvinde A.M., Lignos D.G. (2021). Seismic design of non-dissipative embedded column base connections, *Journal of Constructional Steel Research*, 177: 106417.

Latour M., Piluso V., Rizzano G. (2014). Rotational behaviour of column base plate connections: Experimental analysis and modelling, *Engineering Structures*, 68: 14-23.

Lee D.Y., Goel S.C., Stojadinovic B. (2008a). Exposed column-base plate connections bending about weak axis: I. numerical parametric study, *International Journal of Steel Structures*, 8(1): 11-27.

Lee D.Y., Goel S.C., Stojadinovic B. (2008b). Exposed column-base plate connections bending about weak axis: II. experimental study, *International Journal of Steel Structures*, 8(1): 29-41.

Luzi L., Lanzano G., Felicetta C., D'Amico M. C., Russo E., Sgobba S., Pacor, F., ORFEUS Working Group 5 (2020). Engineering Strong Motion Database (ESM) (Version 2.0). Istituto Nazionale di Geofisica e Vulcanologia (INGV).

Mahin S.A. (1998). Lessons from damage to steel buildings during the Northridge earthquake, *Engineering Structures*, 20(4-6): 261-270.

McKenna F., Scott M.H., Fenves G.L. (2010). Non-linear finite-element analysis software architecture using object composition, *Journal of Computing in Civil Engineering*, 24: 95-107.

Okazaki T., Lignos D.G., Midorikawa M., Ricles J.M., Love J. (2013). Damage to steel buildings observed after the 2011 Tohoku-Oki earthquake. *Earthquake Spectra*, 29(1_suppl): 219-243.

Seco L.D., Couchaux M., Hjiaj M., Neves L.C. (2021). Column base-plates under biaxial bending moment, *Engineering Structures*, 231: 111386.

You Y.C., Lee D. (2020). Effect of anchors on the seismic performance of exposed column-base plate weak-axis connections, *Journal of Building Engineering*, 32: 101803.

Zhou F., Suita K., Matsumiya T., Kurata M. (2004). Tests on steel column bases with t-stub connections, *Journal of Structural and Construction Engineering*, 69(581): 117-125.